

RESEARCH REPORT

Functional analysis of Niemann-Pick disease type C family protein, NPC1a, in *Drosophila melanogaster*

Tzofia Bialistoky^{2,*}, Diane Manry^{1,*}, Peyton Smith¹, Christopher Ng¹, Yunah Kim¹, Sol Zamir², Victoria Moyal², Rachel Kalifa², Paul Schedl¹, Offer Gerlitz^{2,‡} and Girish Deshpande^{1,‡}

ABSTRACT

During embryonic gonad coalescence, primordial germ cells (PGCs) follow a carefully choreographed migratory route circumscribed by guidance signals towards somatic gonadal precursor cells (SGPs). In *Drosophila melanogaster*, SGP-derived Hedgehog (Hh), which serves as a guidance cue for the PGCs, is potentiated by mesodermally restricted HMGCoA-reductase (*Hmgcr*) and the ABC transporter Multi-drug-resistant-49 (*Mdr49*). Given the importance of cholesterol modification in the processing and long-distance transmission of the Hh ligand, we have analyzed the involvement of the Niemann-Pick disease type C-1a (NPC1a) protein, a cholesterol transporter, in germ cell migration and Hedgehog signaling. We show that mesoderm-specific inactivation of *Npc1a* results in germ cell migration defects. Similar to *Mdr49*, PGC migration defects in the *Npc1a* embryos are ameliorated by a cholesterol-rich diet. Consistently, reduction in *Npc1a* weakens the ability of ectopic HMG Coenzyme A reductase (*Hmgcr*) to induce germ cell migration defects. Moreover, compromising *Npc1a* levels influences Hh signaling adversely during wing development, a process that relies upon long-range Hh signaling. Last, doubly heterozygous embryos (*Mdr49/Npc1a*) display enhanced germ cell migration defects when compared with single mutants (*Npc1a/+* or *Mdr49/+*), supporting cooperative interaction between the two.

KEY WORDS: Cell migration, *Drosophila melanogaster*, Embryogenesis, Primordial germ cells

INTRODUCTION

The Hh pathway is one of the most versatile signaling circuitry reiteratively employed in a variety of developmental contexts (Ingham and McMahon, 2001; Jiang and Hui, 2008; Briscoe and Théron, 2013). Hh was first discovered in the genetic screens performed in *Drosophila melanogaster* to uncover the key players during embryonic patterning (Nüsslein-Volhard and Wieschaus, 1980). During embryogenesis, spatially restricted expression of Hh is necessary to regulate downstream targets such as the *Drosophila Wnt1* ortholog Wingless (Wg) in neighboring cells (Perrimon et al., 2012). Detailed molecular genetic analysis has also uncovered a role for Hh signaling in patterning the appendages of the adult fly (Strigini and Cohen, 1997). Hh is expressed along the posterior

compartment boundary of the wing imaginal disc and activates target genes in the anterior compartment to specify the positional identity of cells across the disc (Tabata and Kornberg, 1994; Basler and Struhl, 1994; Struhl et al., 1997).

The multi-pass transmembrane protein encoded by the segment polarity gene *patched* (*ptc*) is the Hh receptor. The binding of Hh ligand to Ptc receptor promotes pathway activation by inhibiting its function. Interestingly, *ptc*[−] embryos display ectopic expression of Hh targets irrespective of Hh activity as Ptc suppresses the signal transduction downstream of Hh by inhibiting Smoothened (Smo). Smo, a member of G-protein-coupled receptor (GPCR) superfamily, is absolutely essential for signal transduction downstream of Hh. Consistently, complete loss of *smo* function eliminates Hh target expression (Alcedo and Noll, 1997; Gallet, 2011). Ptc may participate in transporting lipid moieties that directly or indirectly inhibit Smo activity (Carstea et al., 1997). Consistent with the notion, Ptc protein structure resembles the cholesterol transporter NPC1a.

While Hh primarily functions as a morphogen, it also moonlights as a guidance cue during cell migration in a number of different contexts, including germ cell migration in *Drosophila* embryos (Deshpande et al., 2001; Charron et al., 2003; Yam et al., 2009). The embryonic gonad of *Drosophila* is generated by the coalescence of the somatic gonadal precursor cells (SGPs) and the primordial germ cells (PGCs). Mesodermally derived SGPs are specified in three bilateral clusters in parasegments 10–12 (Jaglarz and Howard, 1994; Boyle and Dinardo, 1995; Boyle et al., 1997). By contrast, the PGCs are formed at the posterior pole of the cellular blastoderm. After internalization post-gastrulation, PGCs migrate through the embryo to reach the mesodermal SGPs. The migratory path of PGCs is determined, in part, by the attractive signals generated by the SGPs (Van doren et al., 1998; Santos and Lehmann, 2004a; Deshpande et al., 2017).

Our earlier ‘gain’- and ‘loss’-of-function studies using specific components of Hh pathway have suggested that *hedgehog* (*hh*) produced by the SGPs functions as an attractant for the migrating PGCs. First, a subset of germ cells mis-migrates towards an ectopic source of Hh ligand. Confirming the idea that PGCs sense the Hh ligand itself, pattern of PGC migration is affected when embryos are maternally compromised for different members of the Hh signal transduction pathway. Importantly, the phenotypic consequences are distinct and reciprocal, depending on the function of the specific component. Embryos maternally compromised for the positive members, such as *smo* (*smo*^{m−}) or *fused* (*fu*^{m−}), display scattering of the PGCs across the mesoderm. By contrast, in the embryos derived from the mothers compromised for the inhibitors of the pathway, such as *ptc* or *Pka*, PGCs clump precociously. This inappropriate clustering of the PGCs is suggestive of premature activation of the Hh pathway.

Taken together, these data argue that Hh functions as a PGC attractant; however, mechanisms underlying specific potentiation of

¹Department of Molecular Biology, Princeton University, Princeton, NJ 08540, USA.

²Developmental Biology and Cancer Research, The Institute for Medical Research Israel-Canada (IMRIC), The Hebrew University-Hadassah Medical School, Jerusalem, Israel.

*These authors contributed equally to this work

‡Authors for correspondence (gdeshpan@princeton.edu; offerg@ekmd.huji.ac.il)

ORCID: O.G., 0000-0002-1574-2088; G.D., 0000-0002-2426-7872

the SGP-derived Hh are still under investigation. Supporting the possibility, we have shown that a number of well documented regulators of germ cell migration, including *Hmgcr*, *qm* and *Fpps*, also function as components of the *hh* signaling pathway (Deshpande et al., 2009, 2013). Moreover, our data suggest that *Hmgcr* helps to mediate the release and/or transport of the Hh ligand emanating from Hh-expressing cells. This is especially relevant as *Hmgcr* expression is not only involved in the production of an SGP-specific attractant but its expression is also progressively restricted to the SGPs (Van doren et al., 1998; Santos and Lehmann, 2004b; Deshpande and Schedl, 2005).

In addition to the *Hmgcr*→isoprenoid biosynthetic pathway, other mechanisms are likely to modulate the production and long-distance signaling activity of Hh. The covalent cholesterol modification plays a crucial role in the intracellular sorting of the processed Hh peptide, and its subsequent release and transmission from basolateral membranes (Porter et al., 1996; Mann and Beachy, 2004; Callejo et al., 2011). Unlike mammals, flies are cholesterol auxotroph (Clayton, 1964; Edwards and Ericsson, 1999). Thus, *hh* signaling would be expected to be sensitive to the levels of dietary cholesterol. The connection between cholesterol, Hh signaling and its potential involvement in germ cell migration is underscored by the discovery of another component of germ cell migration, the ATP-binding cassette (ABC) transporter *Mdr49* (Higgins, 1992; Ricardo and Lehmann, 2009). Although it was postulated that *Mdr49*, which is produced in the mesoderm, assists the release and/or transport of the PGC attractant from the SGPs, these studies did not identify the specific attractant. Employing the 'loss'- and 'gain'-of-function strategies, we showed that *Mdr49* potentiates the signaling activity of the Hh ligand. Consequently, in *Mdr49* mutant embryos, Hh is inappropriately sequestered in the *hh*-expressing cells. Supporting a role for *Mdr49* in providing cholesterol for Hh modification, PGC migration defects in *Mdr49* embryos are ameliorated by a cholesterol-rich diet (Deshpande et al., 2016).

Emboldened by these data, we hypothesized that germ cell behavior may depend upon factors directly responsible for cholesterol transmission. Here, we report involvement of a well-documented cholesterol transporter, NPC1a, in germ cell migration and Hh signaling.

RESULTS AND DISCUSSION

***Drosophila* homolog Niemann-Pick type C-1a mutants confer germ cell migration defects**

Npc1a encodes a membrane-associated protein containing a sterol-sensing domain and is involved in intracellular trafficking of cholesterol (Huang et al., 2005). Mutations in the human ortholog of *Npc1a* cause a neurodegenerative lysosomal storage disorder called Niemann-Pick type C (NPC) disease (Phillips et al., 2008). Similarly, mutations in its *Drosophila* homologs, *Npc1a* and *Npc1b*, confer a homozygous lethal phenotype during larval stages (Fluegel et al., 2006; Voght et al., 2007). Loss of *Npc1a* function results in inappropriate accumulation of cholesterol inclusion bodies in neurons, resulting in neuronal degeneration.

To assess whether *Npc1a* is necessary during germ cell migration, we employed two different mutant alleles: a null allele, *Npc1a^{57A}*, and a partial, loss-of-function allele, *Npc1a^{ep}* (Fig. 1). In *Npc1a* mutant embryos, near normal numbers of PGCs are formed that enter and exit the posterior midgut by stage 10 (Ore-R: mean ~23; *n*=14 V/S NPC1a: mean ~24.7; *n*=12). By stage 13, however, PGCs are not aligned against the SGPs and in several instances they are scattered in the posterior of the embryo (Fig. 1C,D). Embryos from the null allele (*Npc1a^{57A}*) show severe germ cell migration defects, as opposed to those derived from the weak allele (~70% of *Npc1a^{57A}* embryos and ~30% of *Npc1a^{ep}* embryos show five or more mis-migrated germ cells). Thus, loss of *Npc1a* influences germ cell migration adversely. Moreover, *Npc1a* activity does not seem to be required either for specification or for proper migration of the SGPs. We estimated the total number of SGPs by employing

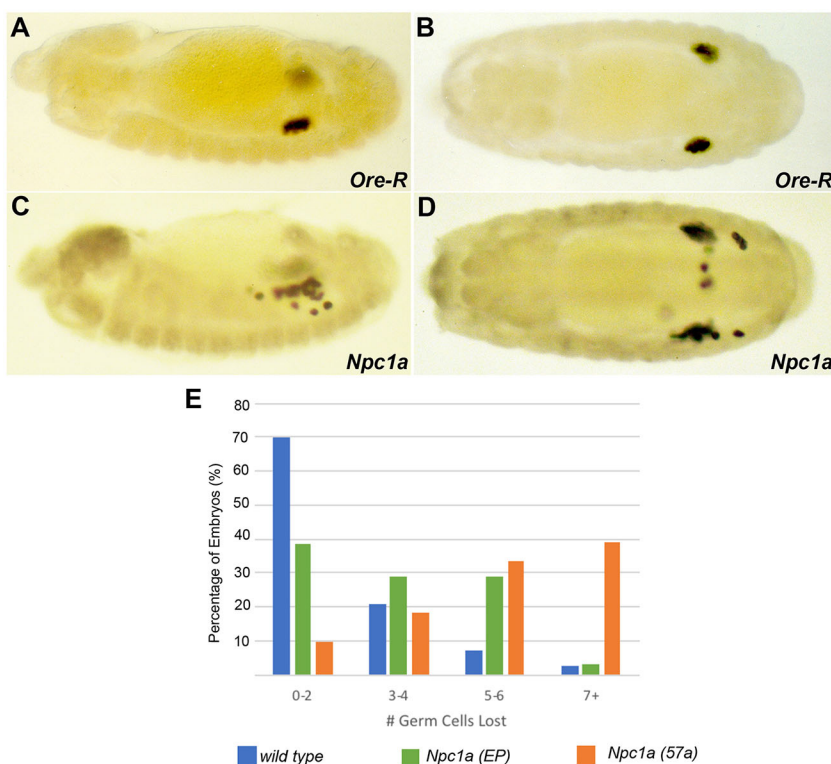


Fig. 1. *Npc1a* is required for embryonic germ cell migration. Embryos of the specified genotypes collected overnight (0-16 h old) were stained with anti-Vasa antibodies to monitor germ cell migration. *Npc1a^{57A}* (null; *n*=72; *P*<0.05) and *Npc1a^{ep}* (weak; *n*=31; *P*<0.05) are two mutant alleles of *Npc1a*. (A,B) Representative Oregon-R control embryos (*n*=43) at stages 13 (A) and 15 (B). (C,D) Two different *Npc1a^{57A}* embryos at stages 13 (C) and 15 (D) with germ cell migration defects. (E) Embryos of different genotypes were classified based on number of mis-migrated PGCs.

anti-Clift specific staining to mark the SGPs. The average number of SGPs varies between 30 and 34 in the coalesced gonads at stage 14/15 (wild-type mean=30.7, $n=8$; *Npc1a* mean=32.6, $n=11$; *UAS Npc1a*-RNAi/ *twist* Gal4 mean=34, $n=7$).

Feeding excess cholesterol to *Npc1a* flies rescues germ cell migration defects induced by the loss of *Npc1a*

The larval lethality of homozygous *Npc1a* mutants can be rescued by raising mutant flies on a cholesterol-rich medium (Fluegel et al., 2006). We therefore wondered whether similar treatment can rescue the embryonic PGC migration defects in the progeny of such mutant adults. Compared with the embryos derived from the *Npc1a* mutant flies raised on normal diet, those derived from the mutant flies raised on cholesterol-rich diet displayed a less severe mutant phenotype. Approximately 70% of *Npc1a* mutant embryos typically have extreme germ cell migration defects (5-7+ lost PGCs). By contrast, only 50% of the embryos from *Npc1a* mutants raised on cholesterol-rich food have extreme germ cell migration defects (Fig. S1B).

To assess whether a long-term feeding method can further improve the extent of rescue, we raised consecutive generations of *Npc1a*/CyO flies on a cholesterol-rich food. The flies resulting from this approach yielded embryos that exhibited a dramatic rescue (Fig. S1C). Almost 75% of the mutant progeny embryos from mutant adults raised on cholesterol-rich diet (vial-fed) showed negligible germ cell migration defects (0-4 germ cells lost; ~55% had lost 0-2). Overall, the offspring of *Npc1a* flies exposed to cholesterol-rich diet exhibit a significant reduction in germ cell migration defects compared with those raised on a normal diet.

Mdr49/*Npc1a* trans-heterozygotes have more-extreme germ cell migration defects than *Mdr49* and *Npc1a* heterozygotes

We have previously shown that germ cell migration defects induced by the loss of *Mdr49* can be substantially ameliorated by raising the flies on a cholesterol-rich diet. Although *Mdr49* and *Npc1a* homozygous mutants display germ cell migration defects, *Mdr49*/+ or *Npc1a*/+ embryos demonstrate no significant deviation from wild type. We sought to examine whether *Mdr49* and *Npc1a* mutations show additive or synergistic interactions during germ cell migration. Thus, we crossed *Npc1a* heterozygous females with *Mdr49* heterozygous males, and screened *Npc1a*/*Mdr49* trans-heterozygous embryos for germ cell migration defects (Fig. S2). More than 55% of trans-heterozygous embryos exhibited significant germ cell migration defects (5-7+ lost PGCs) when compared with 10% defects observed in heterozygous embryos, indicating that simultaneous partial loss of both *Npc1a* and *Mdr49* is sufficient to disrupt germ cell migration (satisfyingly, similar genetic interaction was also observed between *hh* and *NPC1a* mutations; Fig. S2).

Npc1a activity is necessary in the mesoderm for proper germ cell migration

Mdr49 is expressed specifically in the mesoderm and *twist*-GAL4-driven expression of *Mdr49* is sufficient to rescue germ cell migration defects in *Mdr49* embryos (Ricardo and Lehmann, 2009). The genetic interaction between *Mdr49* and *Npc1a* prompted us to assess a mesodermal requirement of *Npc1a*. To manipulate its expression in a cell-type-specific manner, we employed the *UAS*-GAL4-based mis-expression system. *Npc1a* expression was selectively compromised using *twist*-GAL4, a mesoderm-specific driver and *UAS*-*Npc1a* RNAi. *Mdr49*-RNAi was used as a positive control. Embryos mesodermally compromised for *Npc1a* (*twi*-GAL4/*UAS*-*Npc1a*-RNAi) and *Mdr49* (*twi*-GAL4/*UAS*-*Mdr49*-RNAi) showed germ cell migration defects by stage 13, unlike

twi-GAL4/*UAS*-GFP-RNAi embryos (Fig. 2A-C). Thus, inactivation of *Npc1a* in the mesoderm can recapitulate the germ cell migration defects detected in *Npc1a* embryos.

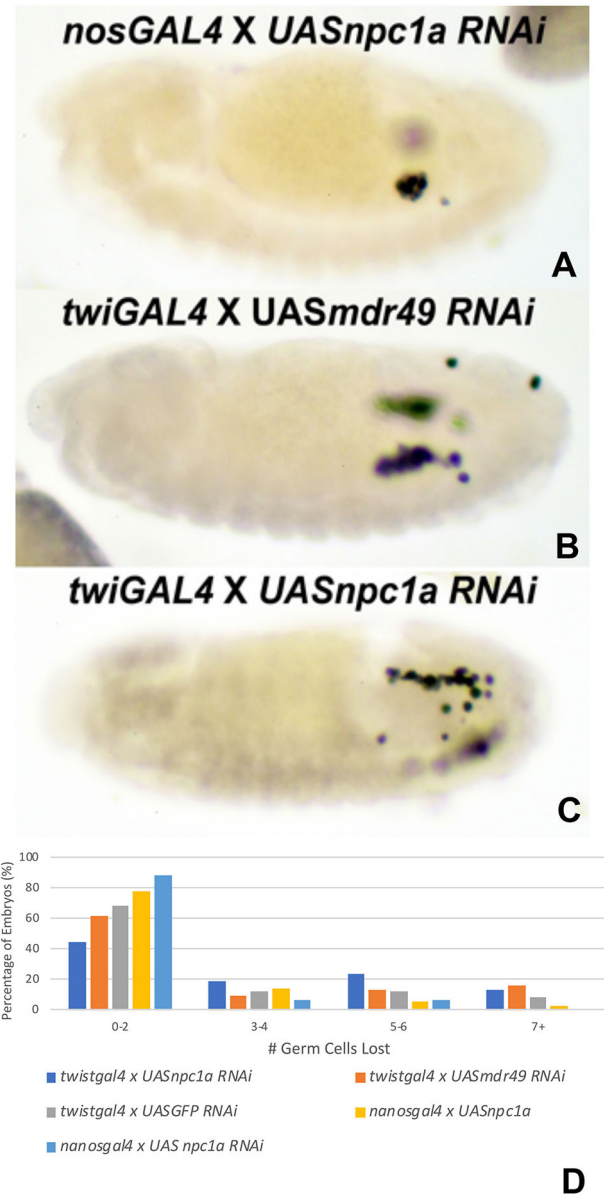


Fig. 2. Mesoderm-specific inactivation of *Npc1a* and *Mdr49* leads to germ cell migration defects. Either mesoderm or PGC-specific expression of different transgenes was achieved by crossing males of specified genotypes with *twist*-Gal4 (mesoderm) or *nanos*-Gal4 (PGC) virgins. Resulting embryos were stained using anti-Vasa antibodies to follow PGC migration. Embryos between stages 13-15 were analyzed to assess the extent of germ cell migration defects. (A) *nanos*-GAL4/*UAS*-*Npc1a*-RNAi. (B) *twist*-GAL4/*UAS*-*Mdr49*-RNAi. (C) *twist*-GAL4/*UAS*-*Npc1a* RNAi. (D) Embryos of appropriate stages from different genotypes were classified based on number of mis-migrated PGCs. Graphical representation shows germ cell migration defects observed in embryos of the following genotypes *twist*-GAL4/*UAS*-*NPC1a*-RNAi ($n=38$; $P<0.05$), *twist*-GAL4/*UAS*-*mdr49*-RNAi ($n=31$; $P<0.05$), *twist*-GAL4/*UAS*-GFP-RNAi ($n=25$), *nanos*-GAL4/*UAS*-*NPC1a* ($n=35$) and *nanos*-GAL4/*UAS*-*NPC1a* RNAi ($n=32$). *twist*-GAL4/*UAS*-GFP-RNAi, *nanos*-GAL4/*UAS*-*NPC1a* and *nanos*-GAL4/*UAS*-*NPC1a* RNAi samples displayed negligible germ cell migration defects that were statistically insignificant ($P>0.3$). (The P values included were generated using *nanos*-GAL4/*UAS*-*Npc1a* RNAi as the control).

By contrast, the pattern of germ cell migration in the *Npc1a*-RNAi X *nanos*-GAL4 embryos was comparable with that of the *twi*-GAL4/*UAS*-GFP-RNAi control. Similarly, germ cell-specific overexpression of *Npc1a* (*nanos*-GAL4×*UAS*-*Npc1a*) did not influence germ cell count or migration behavior (Fig. 2D). Taken together these data suggest that change in *Npc1a* levels in a PGC-specific manner does not influence PGC behavior appreciably.

Next, to test whether restoring *Npc1a* activity can mitigate the effect of *Npc1a*-RNAi expression on germ cell behavior, we simultaneously overexpressed *Npc1a* and *Npc1a*-RNAi in the mesoderm. A significant proportion of *twist*-gal4; *UAS*-*Npc1a*/*UAS*-*Npc1a*-RNAi embryos showed near normal germ cell migration, whereas ~40% of *twi*-GAL4; *UAS*-*Npc1a*-RNAi embryos displayed moderate to severe migration defects (Fig. S3, compare A with B and C). These data establish that mesoderm-specific inactivation of *Npc1a* is responsible for aberrant germ cell migration and that overexpression of *Npc1a* in the mesoderm can ameliorate these defects.

Mutations in *Npc1a* mitigate germ cell migration defects resulting from ectopic expression of *Hmgcr*

Although *Npc1a* appears to be needed in the mesoderm for PGC migration, it was unclear whether it functions in a cell-autonomous manner. To assess whether *Npc1a* functions in the same cell type that generates the germ cell attractant, we decided to examine its ability to influence *Hmgcr* activity. Selective SGP-specific enrichment in *Hmgcr* expression is instrumental in attracting the PGCs towards them. Supporting its involvement in potentiating the attractant, ectopic expression of *Hmgcr* induces severe germ cell migration defects. For example, in *elav*-GAL4 *UAS*-*Hmgcr* embryos, where *Hmgcr* is ectopically expressed in the central nervous system, germ

cells are attracted to both the endogenous source of *Hmgcr* in the mesoderm and the ectopic source of *Hmgcr* in the central nervous system (Ricardo and Lehmann, 2009; Deshpande et al., 2013). As a result, many PGCs end up migrating towards the central nervous system instead of reaching their correct destination, the SGPs.

We were therefore curious whether reducing *Npc1a* activity would weaken the strength of the ectopic source of *Hmgcr*, ultimately resulting in partial suppression of PGC migration defects. Conversely, increasing the expression of *Npc1a* in the CNS should enhance the migration defects due to potentiation of the attractant(s).

To test this hypothesis, *elav*-GAL4 *UAS*-*Hmgcr* recombinant males were crossed with either homozygous *UAS*-*Npc1a*, *UAS*-*Npc1a*-RNAi or *white*¹ (Fig. 3) females. The progeny embryos were assessed for germ cell migration defects. Interestingly, simultaneous ectopic expression of *Hmgcr* and *Npc1a* induced modestly enhanced migration defects when compared with control embryos (*elav*-GAL4 *UAS*-*Hmgcr*×*w*¹). By contrast, the *elav*-GAL4 *UAS*-*Hmgcr*/*UAS*-*Npc1a*-RNAi embryos showed significantly reduced germ cell migration defects (Fig. 3). Taken together, these data demonstrate that germ cell migration defects induced by the ectopic *Hmgcr* expression are sensitive to levels/activity of *Npc1a*. In this regard, *Npc1a* appears to behave similarly to *Mdr49* and likely is required in cells that synthesize the PGC attractant (Ricardo and Lehmann, 2009).

Reducing *Npc1a* in the developing wing attenuates Hh signaling

We have previously shown that *Hmgcr* and *Mdr49* can influence the range/strength of Hh signaling, possibly via enhancing the transmission of Hh ligand. Importantly, such an effect was even

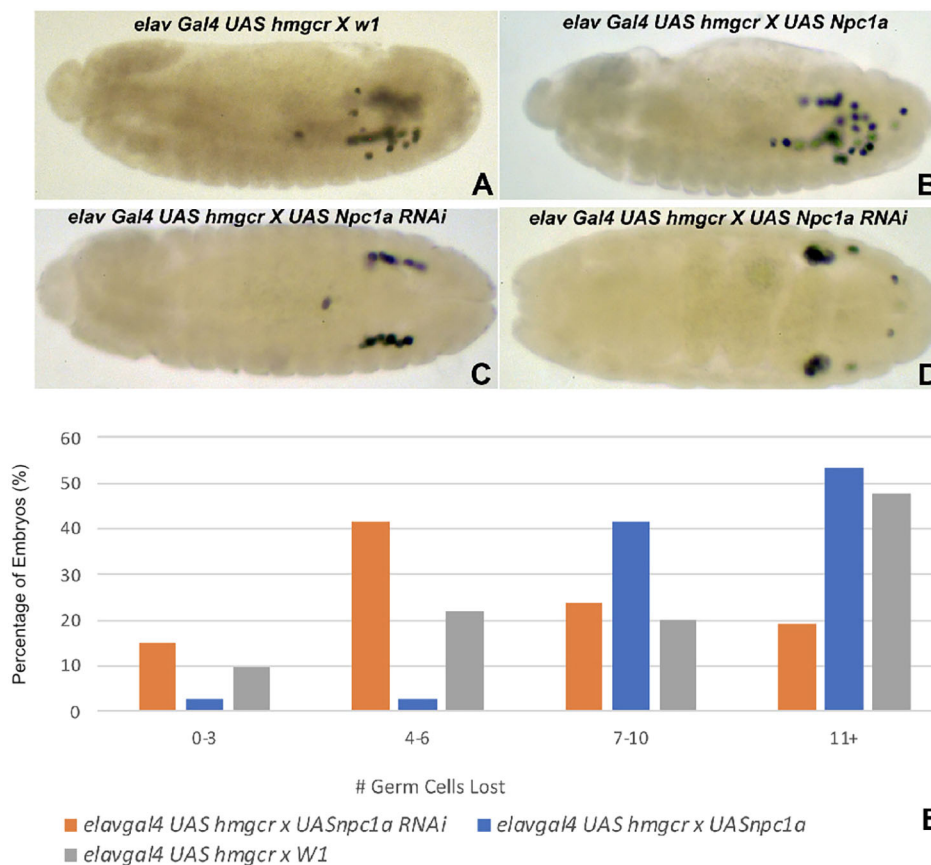


Fig. 3. Germ cell migration defects induced by ectopic expression of *Hmgcr* are sensitive to levels of *Npc1a*. Ectopic expression of *Hmgcr* in the central nervous system (CNS), driven by *elav*-GAL4 induces germ cells to migrate towards the CNS. Migration defects were visualized and quantified in the embryos of specified genotypes at stages 13-15. (A) *elav-gal4 UAS-Hmgcr*×*w*¹ (n=50). (B) *elav-gal4 UAS-Hmgcr*×*UAS-Npc1a* (n=77; *P*<0.0005). (C,D) *elav-gal4 UAS-Hmgcr*×*UAS-Npc1a*-RNAi (n=67; *P*<0.01). Top view of the embryos is shown to demonstrate dramatic rescue. Image in C is stage 13; image in D is stage 15. (E) Graphical representation of germ cell migration defects in different genotypes.

observed in *Hmgcr*^{Z-} and *Mdr49*^{Z-} embryos. (Z⁻ refers to the homozygous mutant embryos derived from the mutant/Balancer stock. Such embryos still have half the level of maternal product.) As *Npc1a* activity seems to contribute to germ cell migration in conjunction with *Mdr49* and *hh*, we wondered whether *Npc1a* also contributes to Hedgehog signaling. However, unlike *Hmgcr*^{Z-} and *Mdr49*^{Z-} embryos, *Npc1a*^{Z-} embryos displayed normal levels of Hh target genes (*wg*, *en*) in the embryonic ectoderm (Fig. S4). The absence of an obvious phenotype could be due to maternal deposition and stability of the *Npc1a* protein. We therefore decided to compromise *Npc1a* levels in the imaginal discs.

In *Drosophila* wing discs, expression of Hh is restricted to the posterior compartment. Hh organizes patterning of the anterior-posterior compartments of the adult wing blade by inducing the expression of downstream targets such as *patched* (*ptc*) and *decapentaplegic* (*dpp*) in the anterior compartment. In the absence of *hh* signaling, these target genes are not activated and there are patterning and growth defects along the anterior-posterior (A-P) axis (Chen and Struhl, 1996; Mullor et al., 1997; Strigini and Cohen, 1997).

To examine whether a reduction in *Npc1a* results in compromised Hh signaling, we knocked down the expression of *Npc1a* using a wing pouch-specific *nubbin-GAL4* driver in combination with *UAS-Npc1a-RNAi*. Upon staining the wing discs using anti-Patched antibody, the experimental wing discs (*nubbin-GAL4; UAS-GFP*) showed a readily detectable reduction in Ptc when compared with the control wing discs (driver alone) (Fig. 4). These data support the claim that Hh signaling is attenuated in wing discs compromised for *Npc1a* activity. Furthermore, the *nubbin-GAL4; UAS-Npc1a-RNAi* wing discs also exhibited significant reduction in both *patched* and *dpp* transcript levels (Fig. 4F) when compared with the control. As *ptc* and *dpp* are biologically relevant targets of Hh morphogen during

wing disc patterning, these data strongly support the claim that Hh signaling is attenuated in wing discs compromised for *Npc1a* activity.

The central region of the *Drosophila* wing spanning the anterior L3 vein, the posterior L4 vein and the L3-L4 intervein region is directly specified by Hh signaling. The length of the anterior cross vein (ACV) adjoining L3 and L4 veins is highly responsive to changes in either Hh activity or the levels of the downstream target Collier/Knot (Crozatier et al., 2002). To assess whether the observed reduction in Hh signaling (Ptc levels) leads to phenotypic consequences, we examined the wings of adult flies. Indeed, compromising *Npc1a* in the wing disc proper using *nubbin-GAL4* resulted in significant reduction in the length of the ACV (Fig. S5).

In summary, to assess whether PGC migration in *Drosophila* embryos is sensitive to cholesterol levels, we focused our attention on a cholesterol transporter, NPC1a, and its connection to both Hh signaling and PGC migration. In flies and in mammals, covalent cholesterol modification of the Hh ligand plays a crucial role in the intracellular sorting of the processed Hh peptide, and its subsequent transmission and release from basolateral membranes. Our data indicate that *Npc1a* likely contributes to generation of sufficient levels of functional cholesterol-modified Hh. Consistently, loss of *Npc1a* can mimic partial loss of Hh activity in adult wings and also leads to a consistent reduction in transcript levels of canonical Hh target genes. Importantly, involvement of NPC1a in Hh signaling appears to be conserved because in *Npc1*-deficient mice, subcellular localization of Shh effectors and ciliary proteins is abrogated. Moreover, in NPC1-deficient mouse brains and the human fibroblasts of individuals with NPC1, the aberrant Shh signaling is correlated with diminished cilia length and the total number of ciliated cells (Canterini et al., 2017). Together, these observations support a novel functional connection between Hh signaling and NPC1a activity.

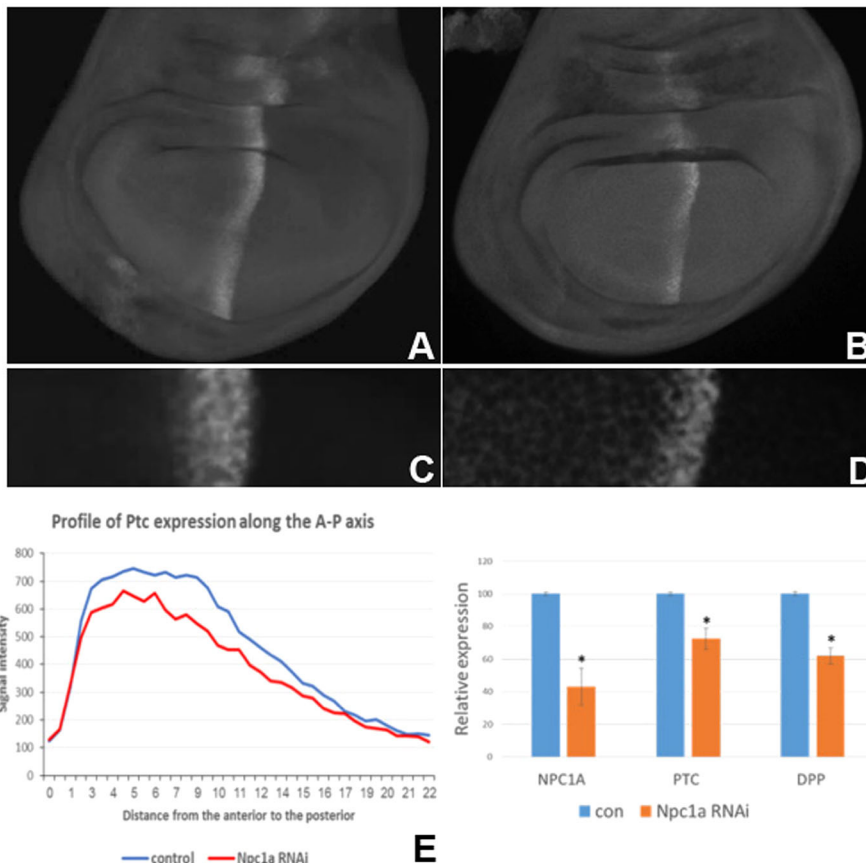


Fig. 4. Reduction in *Npc1a* activity leads to a decrease in the Hh targets *ptc* and *dpp*. *UAS-dicer; nub-Gal4* flies were mated with *UAS-Npc1a-RNAi* flies. (A,B) Wing discs from the third instar progeny larvae were fixed and stained using anti-Ptc antibodies. The panels show representative wing discs. In both panels, anterior is to the left. (A) *UAS-dicer; nubbin-Gal4; UAS-GFP* (control). (B) *UAS-dicer; nubbin-Gal4/UAS-Npc1a-RNAi; UAS-Npc1a-RNAi*. (C,D) Magnified views of A and B, respectively. (E) Graphical representation of the decrease in Ptc expression across the anterior-posterior axis of wing discs. Both the intensity and the spread of Ptc are reduced in the experimental samples ($n=72$) compared with the control ($n=93$). Thirty randomly selected wing discs from both the genotypes were used to estimate the area under graph in Excel (control mean: 10835.27; NPC1a RNAi mean: 8498.565; $P=0.002248$). (F) Graphical representation of the decrease in the expression levels of Hh target genes following *Npc1a* knockdown. RT-qPCR analysis of *Npc1a*, *ptc* and *dpp* mRNA expression levels in wing discs of control (blue) and *Npc1a* KD (orange) third instar larvae. * $P<0.05$. Statistical significance was determined using a two-tailed Student's *t*-test.

Future experiments will determine whether NPC1a is directly responsible for Hh transmission and whether compromised Hh signaling contributes to Niemann-Pick disease symptoms.

MATERIALS AND METHODS

Immunohistochemistry in embryos

Embryo collection and staining were performed essentially as described previously (Deshpande et al., 2013). Vasa (from Paul Lasko, McGill University, Canada) and Hh (from Tom Kornberg, University of California, San Francisco, USA) antibodies are rabbit polyclonal antibodies. Both were used at 1:500 dilution. Engrailed and Wingless antibodies (Developmental Studies Hybridoma Bank) are mouse monoclonal antibodies and were used at 1:10 dilution. β -Galactosidase antibody was either a rabbit polyclonal [MP Biomedicals (previously Cappel), 55976; 1:1000] or a mouse monoclonal antibody (Developmental Studies Hybridoma Bank; 1:10). GFP antibody was a rabbit polyclonal (Torrey Pines Biolabs, ABIN2562810; 1:1000). Secondary antibodies were purchased from Molecular Probes and used at 1:500. For confocal analysis, 40 \times magnification was used in almost all the analysis, and images were collected using identical settings for the control and experimental samples on a Nikon A1 microscope with GaAsP detectors.

Immunohistochemistry

Imaginal discs from third instar larvae were fixed and stained using standard techniques (Callejo et al., 2011). The specific primary antibodies used were: mouse anti-Ptc [1:100; DSHB *Drosophila* Ptc (Apa 1)-s]. Secondary antibodies were conjugated with Rhodamine Red-X (1:400; Jackson Labs). Images were captured on an A1R confocal microscope (Nikon). Figures were edited using Adobe Photoshop 7.0. Data were analyzed using Nis Elements software.

Mutant and misexpression analysis

Fly stocks were raised at 25°C, on standard medium and were primarily obtained from the *Drosophila* FlyBase (Bloomington, IN, USA). Alleles used in the *npc1a* experiments are as follows: *npc1a*^{57A} and *npc1a*^{Scer\UAS, T:Avic\GFP-EYFP}. The *npc1a*^{ep1} refers to the *npc1a*^{Scer\UAS, T:Avic\GFP-EYFP} allele. In the *npc1a* RNAi ectopic expression experiment, virgin females homozygous for the transgene *UAS npc1a* RNAi, *UAS Mdr49* RNAi or *UAS GFP* RNAi were crossed with males homozygous for the transgene *twist-GAL4* or *nanos-GAL4*. *Gyl* mutant stocks, *Gyl*^{N159} and *Gyl*^{k0817}, were obtained from Fumio Matsuzaki (RIKEN Center for Developmental Biology, Kobe, Japan). The *Mdr49* mutants and overexpression stocks were obtained from Ruth Lehmann (Skirball Biomedical Institute, NYU, USA). The *UAS*-RNAi lines specific for *Mdr49* (Bloomington, 32405) and *Gal4* stocks used for the misexpression studies were from the Bloomington Stock Center (*patched-Gal4*, *UAS- β -galactosidase* and *hh-Gal4/TM6 Ubx-lacZ*). In most experiments, males carrying two copies of the *UAS* transgene were mated with virgin females carrying two copies of the *Gal4* transgene. Embryos derived from the cross were fixed and stained for subsequent analysis. The genotypes of the embryos were unambiguously determined by using the balancer chromosomes marked with either GFP or β -galactosidase. The following stocks were used for analysis of wing discs: *UAS-GFP* (Bloomington, 1522), *UAS-dicer-2*; *nub-Gal4* (Bloomington, 25754) and *UAS npc1a* RNAi; *UAS npc1a* RNAi (VDRC, 42782; Bloomington, 37504). Transgenes were expressed using the *Gal4-UAS* binary system.

qRT-PCR

Total RNA was isolated from third instar larval wing discs (~30 for each sample) of *UAS-dicer*; *nub-Gal4*; *UAS-GFP* (control) and *npc1a* RNAi KD; *UAS-dicer*; *nub-Gal4/UAS-npc1a* RNAi; *UAS-npc1a* RNAi (experimental) using the QIAGEN RNeasy mini kit. Briefly, wandering third instar larvae were collected, males were selected and dissected in chilled 1 \times PBS. For each wing disc, the notum was removed. The pouch and hinge tissue were collected in the lysis buffer. Total RNA was extracted as per the manufacturer's instructions. cDNA was made using the high-capacity cDNA reverse transcription kit (Applied Biosystems) using an

equal amount of total RNA from each sample. Real-time q-PCR analyses were carried out using the Powersyber Green PCR Master Mix and QuantStudio 12k flex (Applied Biosystems). Rp49 and TBP served as reference genes. Each sample was analyzed in triplicate; the results were confirmed by at least two independent experiments.

Primer sequences used for qPCR were: RP49-F, 5'-TAAGCTGTGCGC-ACAAATGGC-3'; RP49-R, 5'-CCGTAACCGATGTTGGGCAT-3'; TBP-F, 5'-GGCAAAGAGTGAGGACGACT-3'; TBP-R, 5'-GTCGAGGAAC-TTTCAGGGA-3'; npc1a-F, 5'-TCATCGAAACAGGACTGCGT-3'; npc1a-R, 5'-ACCGTCAGTTGCCATTTCT-3'; ptc primer set 1-F, 5'-T-ACGGAGCTTCTCAGGGCAA-3'; ptc primer set 1-R, 5'-CCAATGGC-AGACTCTTGGGT-3'; ptc primer set 2-F, 5'-CACCTCATTCGCTGCTCG-AT-3'; ptc primer set 2-R, 5'-GAGGCCTGGTATAACGACCG-3'; dpp-F, 5'-GCCAACACAGTGCGAAGTTT-3'; and dpp-R, 5'-GTGGCGGG AATGCTCTT-3'.

Cholesterol feeding assay

Drosophila food containing cholesterol was prepared as described previously (Fluegel et al., 2006). Cholesterol (Sigma) was used to prepare a stock solution (30 mg/ml) in ethanol. The final concentration was 200 ng/ml. To achieve uniform dispersion of cholesterol, food was mixed thoroughly after cooling it down to 65°C before pouring into either vials or bottles.

Quantifying germ cell migration

Embryos between stages 13 and 15 of a given genotype were analyzed, and the number of germ cells accounted for were the germ cells that showed deviation from the location of the somatic gonadal precursor cells at these stages. For each genotype, the number of embryos examined is indicated in the corresponding graph legend. All staining experiments were repeated three times and statistical significance was estimated using standard two-tailed *t*-test.

Cholesterol feeding

Flies that were 'cholesterol-fed' were fed yeast that was mixed with cholesterol, as opposed to just yeast during the time of egg laying and collection. The cholesterol powder was purchased from Sigma and was dissolved in acetone. The yeast paste was mixed with the cholesterol solution (200 μ g/ml) to give a final concentration of 200 ng/ml. Flies that were 'vial-fed' were fed according to the procedure described by Fluegel et al. (2016). *npc1a*^{+/+} flies were fed food that contained 200 ng/ml cholesterol for 6 days. These flies were then placed on plates where they ate cholesterol-rich food for egg lay and collection.

Acknowledgements

For antibodies and stocks, we acknowledge the Developmental Studies Hybridoma Bank, Drs P. Lasko, T. Kornberg, I. Guerrero, R. Lehmann, F. Matsuzaki, E. Olson and the Bloomington Stock Center. We also thank Eric Wieschaus and Trudi Schupbach for helpful discussions and overall encouragement. We thank Dr Gary Laevsky and the Molecular Biology Confocal Microscopy Facility, which is a Nikon Center of Excellence. Gordon Grey provided fly media. We thank Ronit Sionov and Eliran Kadosh for assisting with the qPCR.

Competing interests

The authors declare no competing or financial interests.

Author contributions

Conceptualization: G.D.; Methodology: O.G., G.D.; Validation: G.D.; Formal analysis: R.K., G.D.; Investigation: T.B., D.M., P. Smith, C.N., Y.K., S.Z., V.M., R.K., O.G., G.D.; Writing - original draft: T.B., O.G., G.D.; Writing - review & editing: D.M., Y.K., R.K., P. Schedl, O.G., G.D.; Supervision: R.K., P. Schedl, O.G., G.D.; Funding acquisition: R.K., P. Schedl, O.G., G.D.

Funding

This work was supported by the National Institutes of Health (HD093913 to P.S. and G.D.). P.S. is a recipient of a Ministry of Education and Science of the Russian Federation grant (14.B25.31.0022). The Israel Science Foundation (960/13) and the Legacy Heritage Bio-Medical Program of the Israel Science Foundation (1788/15) supported the research in the Gerlitz laboratory. Deposited in PMC for release after 12 months.

Supplementary information

Supplementary information available online at
<http://dev.biologists.org/lookup/doi/10.1242/dev.168427.supplemental>

References

- Alcedo, J. and Noll, M.** (1997). Hedgehog and its patched-smoothened receptor complex: a novel signaling mechanism at the cell surface. *Biol. Chem.* **378**, 583-590.
- Basler, K. and Struhl, G.** (1994). Compartment boundaries and the control of Drosophila limb pattern by Hedgehog protein. *Nature* **368**, 208-214. doi:10.1038/368208a0
- Boyle, M. and Dinardo, S.** (1995). Specification, migration and assembly of the somatic-cells of the Drosophila gonad. *Development* **121**, 1815-1825.
- Boyle, M., Bonini, N. and DiNardo, S.** (1997). Expression and function of clift in the development of somatic gonadal precursors within the Drosophila mesoderm. *Development* **124**, 971-982.
- Briscoe, J. and Théron, P.** (2013). The mechanisms of Hedgehog signalling and its roles in development and disease. *Nat. Rev. Mol. Cell Biol.* **14**, 418-431. doi:10.1038/nrm3598
- Callejo, A., Bilioni, A., Mollica, E., Gorfinkiel, N., Andrés, G., Ibáñez, C., Torroja, C., Doglio, L., Sierra, J. and Guerrero, I.** (2011). Dispatched mediates Hedgehog basolateral release to form the long-range morphogenetic gradient in the Drosophila wing disk epithelium. *Proc. Natl. Acad. Sci. USA* **108**, 12591-12598. doi:10.1073/pnas.1106881108
- Canterini, S., Dragotto, J., Dardis, A., Zampieri, S., De Stefano, M. E., Mangia, F., Erickson, R. P. and Fiorenza, M. T.** (2017). Shortened primary cilium length and dysregulated Sonic hedgehog signaling in Niemann-Pick C1 disease. *Hum. Mol. Genet.* **26**, 2277-2289. doi:10.1093/hmg/ddx118
- Carstea, E. D., Morris, J. A., Coleman, K. G., Loftus, S. K., Zhang, D., Cummings, C., Gu, J., Rosenfeld, M. A., Pavan, W. J., Krizman, D. B. et al.** (1997). Niemann-Pick C1 disease gene: homology to mediators of cholesterol homeostasis. *Science* **277**, 228-231. doi:10.1126/science.277.5323.228
- Charron, F., Stein, E., Jeong, J., McMahon, A. and Tessier-Lavigne, M.** (2003). The morphogen sonic hedgehog is an axonal chemoattractant that collaborates with netrin-1 in midline axon guidance. *Cell* **113**, 11-23. doi:10.1016/S0092-8674(03)00199-5
- Chen, Y. and Struhl, G.** (1996). Dual roles for patched in sequestering and transducing Hedgehog. *Cell* **87**, 553-563. doi:10.1016/S0092-8674(00)81374-4
- Clayton, R.** (1964). The utilization of sterols by insects. *J. Lipid Res.* **15**, 3-19.
- Crozatier, M., Glise, B. and Vincent, A.** (2002). Connecting Hh, Dpp and EGF signalling in patterning of the Drosophila wing: the pivotal role of collier/knot in the AP organiser. *Dev. Camb. Engl.* **129**, 4261-4269.
- Deshpande, G. and Schedl, P.** (2005). HMGCoA reductase potentiates hedgehog signaling in Drosophila melanogaster. *Dev. Cell* **9**, 629-638. doi:10.1016/j.devcel.2005.09.014
- Deshpande, G., Swanhart, L., Chiang, P. and Schedl, P.** (2001). Hedgehog signaling in germ cell migration. *Cell* **106**, 759-769. doi:10.1016/S0092-8674(01)00488-3
- Deshpande, G., Godishala, A. and Schedl, P.** (2009). G gamma 1, a downstream target for the *hmgcr*-isoprenoid biosynthetic pathway, is required for releasing the hedgehog ligand and directing germ cell migration. *PLoS Genet.* **5**, e1000333. doi:10.1371/journal.pgen.1000333
- Deshpande, G., Zhou, K., Wan, J. Y., Friedrich, J., Jourjine, N., Smith, D. and Schedl, P.** (2013). The hedgehog pathway gene shifted functions together with the *hmgcr*-dependent isoprenoid biosynthetic pathway to orchestrate germ cell migration. *PLoS Genet.* **9**, e1003720. doi:10.1371/journal.pgen.1003720
- Deshpande, G., Manry, D., Jourjine, N., Mogila, V., Mozes, H., Bialistok, T., Gerlitz, O. and Schedl, P.** (2016). Role of the ABC transporter Mdr49 in Hedgehog signaling and germ cell migration. *Dev. Camb. Engl.* **143**, 2111-2120. doi:10.1242/dev.133587
- Deshpande, G., Barr, J., Gerlitz, O., Lebedeva, L., Shidlovskii, Y. and Schedl, P.** (2017). Cells on the move: modulation of guidance cues during germ cell migration. *Fly (Austin)* **11**, 200-207. doi:10.1080/19336934.2017.1304332
- Edwards, P. A. and Ericsson, J.** (1999). Sterols and isoprenoids: signaling molecules derived from the cholesterol biosynthetic pathway. *Annu. Rev. Biochem.* **68**, 157-185. doi:10.1146/annurev.biochem.68.1.157
- Fluegel, M. L., Parker, T. J. and Pallanck, L. J.** (2006). Mutations of a Drosophila NPC1 gene confer sterol and ecdysone metabolic defects. *Genetics* **172**, 185-196. doi:10.1534/genetics.105.046565
- Gallet, A.** (2011). Hedgehog morphogen: from secretion to reception. *Trends Cell Biol.* **21**, 238-246. doi:10.1016/j.tcb.2010.12.005
- Higgins, C. F.** (1992). ABC transporters: from microorganisms to man. *Annu. Rev. Cell Biol.* **8**, 67-113. doi:10.1146/annurev.cb.08.110192.000435
- Huang, X., Suyama, K., Buchanan, J., Zhu, A. J. and Scott, M. P.** (2005). A Drosophila model of the Niemann-Pick type C lysosome storage disease: *dnpc1a* is required for molting and sterol homeostasis. *Development* **132**, 5115-5124. doi:10.1242/dev.02079
- Ingham, P. W. and McMahon, A. P.** (2001). Hedgehog signaling in animal development: paradigms and principles. *Genes Dev.* **15**, 3059-3087. doi:10.1101/gad.938601
- Jaglarz, M. K. and Howard, K. R.** (1994). Primordial germ cell migration in Drosophila melanogaster is controlled by somatic tissue. *Development* **120**, 83-89.
- Jiang, J. and Hui, C.-C.** (2008). Hedgehog signaling in development and cancer. *Dev. Cell* **15**, 801-812. doi:10.1016/j.devcel.2008.11.010
- Mann, R. K. and Beachy, P. A.** (2004). Novel lipid modifications of secreted protein signals. *Annu. Rev. Biochem.* **73**, 891-923. doi:10.1146/annurev.biochem.73.011303.073933
- Muller, J. L., Calleja, M., Capdevila, J. and Guerrero, I.** (1997). Hedgehog activity, independent of decapentaplegic, participates in wing disc patterning. *Dev. Camb. Engl.* **124**, 1227-1237.
- Nüsslein-Volhard, C. and Wieschaus, E.** (1980). Mutations affecting segment number and polarity in Drosophila. *Nature* **287**, 795-801. doi:10.1038/287795a0
- Perrimon, N., Pitsouli, C. and Shilo, B.-Z.** (2012). Signaling mechanisms controlling cell fate and embryonic patterning. *Cold Spring Harb. Perspect. Biol.* **4**, a005975. doi:10.1101/cshperspect.a005975
- Phillips, S. E., Woodruff, E. A., Liang, P., Patten, M. and Broadie, K.** (2008). Neuronal loss of Drosophila NPC1a causes cholesterol aggregation and age-progressive neurodegeneration. *J. Neurosci. Off. J. Soc. Neurosci.* **28**, 6569-6582. doi:10.1523/JNEUROSCI.5529-07.2008
- Porter, J. A., Ekker, S. C., Park, W.-J., von Kessler, D. P., Young, K. E., Chen, C.-H., Ma, Y., Woods, A. S., Cotter, R. J., Koonin, E. V. et al.** (1996). Hedgehog patterning activity: role of a lipophilic modification mediated by the carboxy-terminal autoprocessing domain. *Cell* **86**, 21-34. doi:10.1016/S0092-8674(00)80074-4
- Ricardo, S. and Lehmann, R.** (2009). An ABC transporter controls export of a Drosophila germ cell attractant. *Science* **323**, 943-946. doi:10.1126/science.1166239
- Santos, A. C. and Lehmann, R.** (2004a). Germ cell specification and migration in Drosophila and beyond. *Curr. Biol.* **14**, R578-R589. doi:10.1016/j.cub.2004.07.018
- Santos, A. C. and Lehmann, R.** (2004b). Isoprenoids control germ cell migration downstream of HMGCoA reductase. *Dev. Cell* **6**, 283-293. doi:10.1016/S1534-5807(04)00023-1
- Strigini, M. and Cohen, S. M.** (1997). A Hedgehog activity gradient contributes to AP axial patterning of the Drosophila wing. *Dev. Camb. Engl.* **124**, 4697-4705.
- Struhl, G., Barbash, D. A. and Lawrence, P. A.** (1997). Hedgehog organises the pattern and polarity of epidermal cells in the Drosophila abdomen. *Development* **124**, 2143-2154.
- Tabata, T. and Kornberg, T. B.** (1994). Hedgehog is a signaling protein with a key role in patterning Drosophila imaginal discs. *Cell* **76**, 89-102. doi:10.1016/0092-8674(94)90175-9
- Van Doren, M., Moore, L. A., Broihier, H. T. and Lehmann, R.** (1998). HMG-CoA reductase guides migrating primordial germ cells. *Nature* **396**, 466-469. doi:10.1038/24871
- Voght, S. P., Fluegel, M. L., Andrews, L. and Pallanck, L. J.** (2007). Drosophila NPC1b promotes an early step in sterol absorption from the midgut epithelium. *Cell Metab.* **5**, 195-205. doi:10.1016/j.cmet.2007.01.011
- Yam, P. T., Langlois, S. D., Morin, S. and Charron, F.** (2009). Sonic hedgehog guides axons through a noncanonical, Src-family-kinase-dependent signaling pathway. *Neuron* **62**, 349-362. doi:10.1016/j.neuron.2009.03.022

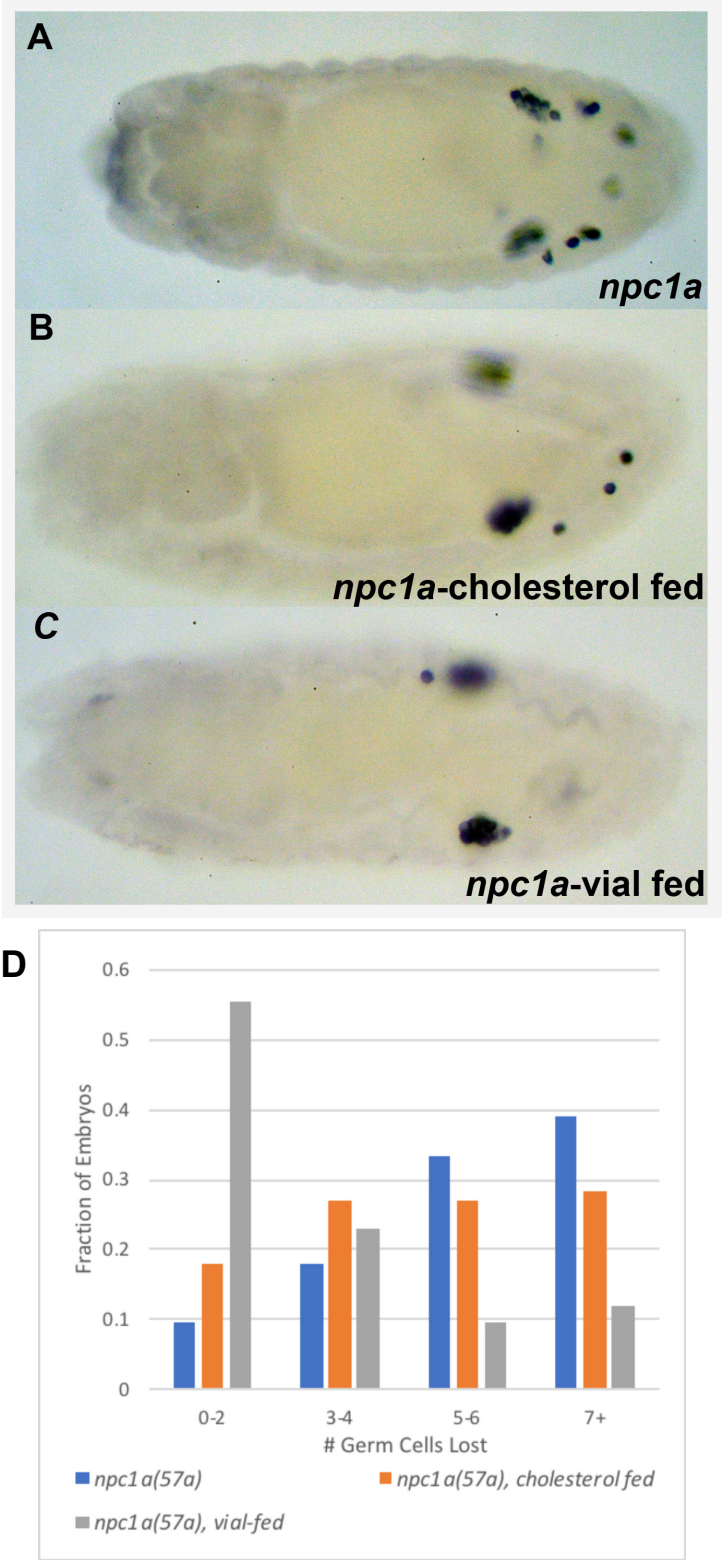


Figure S1. Cholesterol rich diet can rescue *NPC1a* mutant phenotype.

Embryos carrying mutant *NPC1a* allele raised on normal diet and cholesterol-rich diet in two different ways were screened for germ cell migration defects. The parents of “vial-fed” embryos were fed excess cholesterol for a longer period of time than those of “cholesterol-fed” embryos. Consistently vial-fed *NPC1a* embryos had the least defects. Embryos between stages 13-15 were analyzed.

(A): *NPC1a*^{57A} (n=72).

(B): *NPC1a* embryo derived from ‘cholesterol-fed’ parents (n=364; p<0.05).

(C): *NPC1a*^{57A} embryo derived from ‘vial-fed’ parents at stage 15 with 1 mis-migrated cells (n=83; p<0.005).

(D): Distribution of germ cell migration defects in *NPC1a*^{57A}, cholesterol fed *NPC1a*^{57A} embryos, and vial-fed *NPC1a*^{57A} embryos.

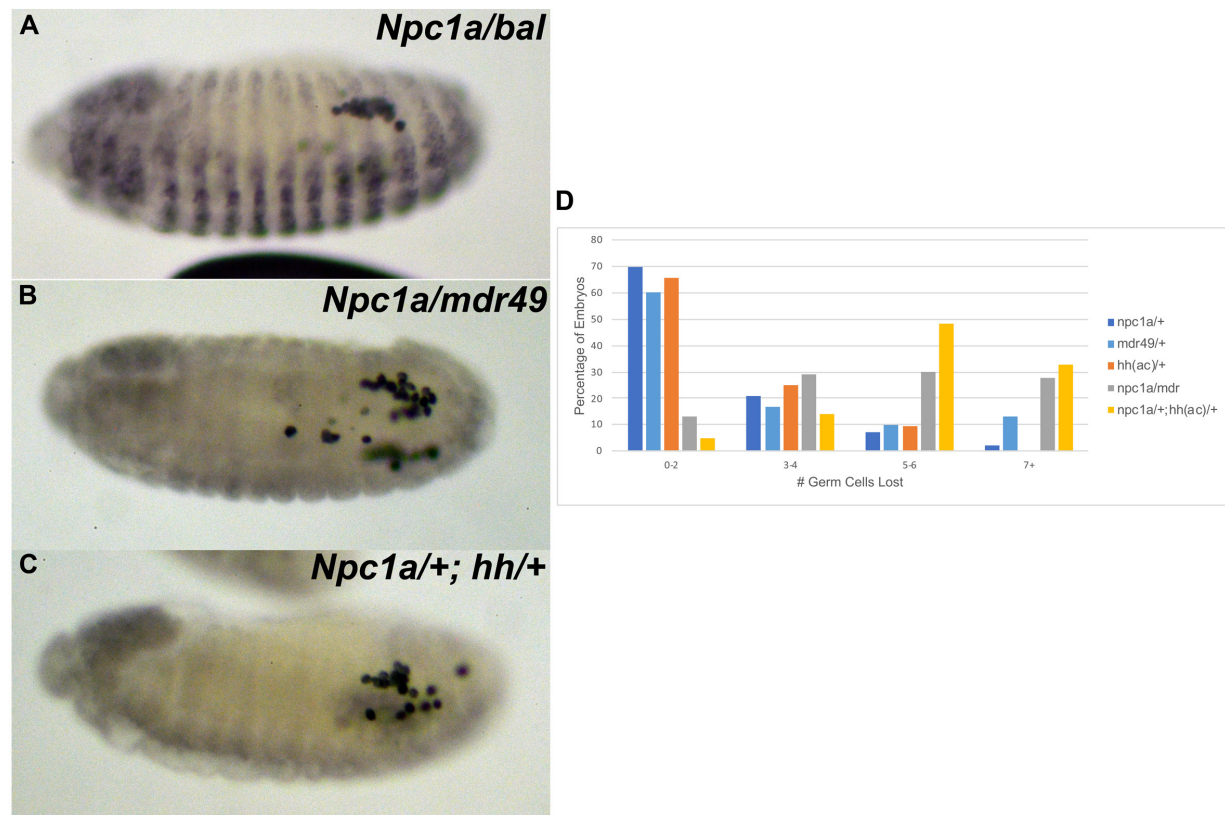


Figure S2. Genetic interaction between *NPC1a* and *mdr49* or *hh* during germ cell migration.

Embryos between stages 13–15 of the indicated genotype were stained with anti-Vasa and β -galactosidase antibody. Total number of germ cells that failed to coalesce and remained scattered were counted per embryo. Nearly 70% of *NPC1a*/+ embryos show 0–2 lost germ cells (blue and red bars respectively). But when embryos are simultaneously compromised for both *NPC1a* and *mdr49* or *hh*, ~ 60% of the embryos have 5 or more lost germ cells.

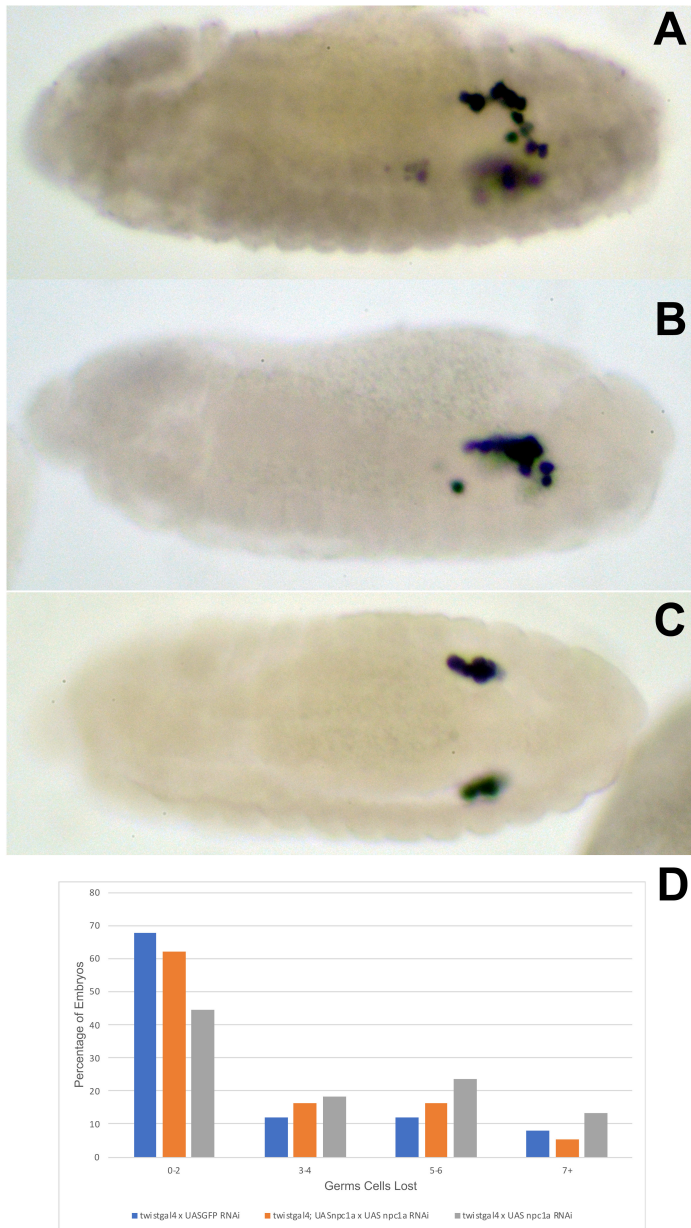


Figure S3. Overexpression of *NPC1a* can rescue aberrant germ cell migration induced by mesodermal inactivation of *NPC1a*.

Simultaneous expression of *UAS-NPC1a* and *UAS-NPC1a RNAi* in the embryonic mesoderm mitigates the germ cell migration defects induced by *NPC1aRNAi*.

(A): *twist-GAL4*; *UAS-NPC1a-RNAi* (n=38; $p < 0.05$).

(B) and (C): *twist-GAL4*; *UAS-NPC1a/UAS-NPC1a-RNAi* (n=37; **The difference between control and the 'rescued' sample is statistically insignificant ($p > 0.1$) indicating the specific and efficient nature of the rescue.**)

(D): Comparison of germ Cell migration defects observed in the two genotypes.

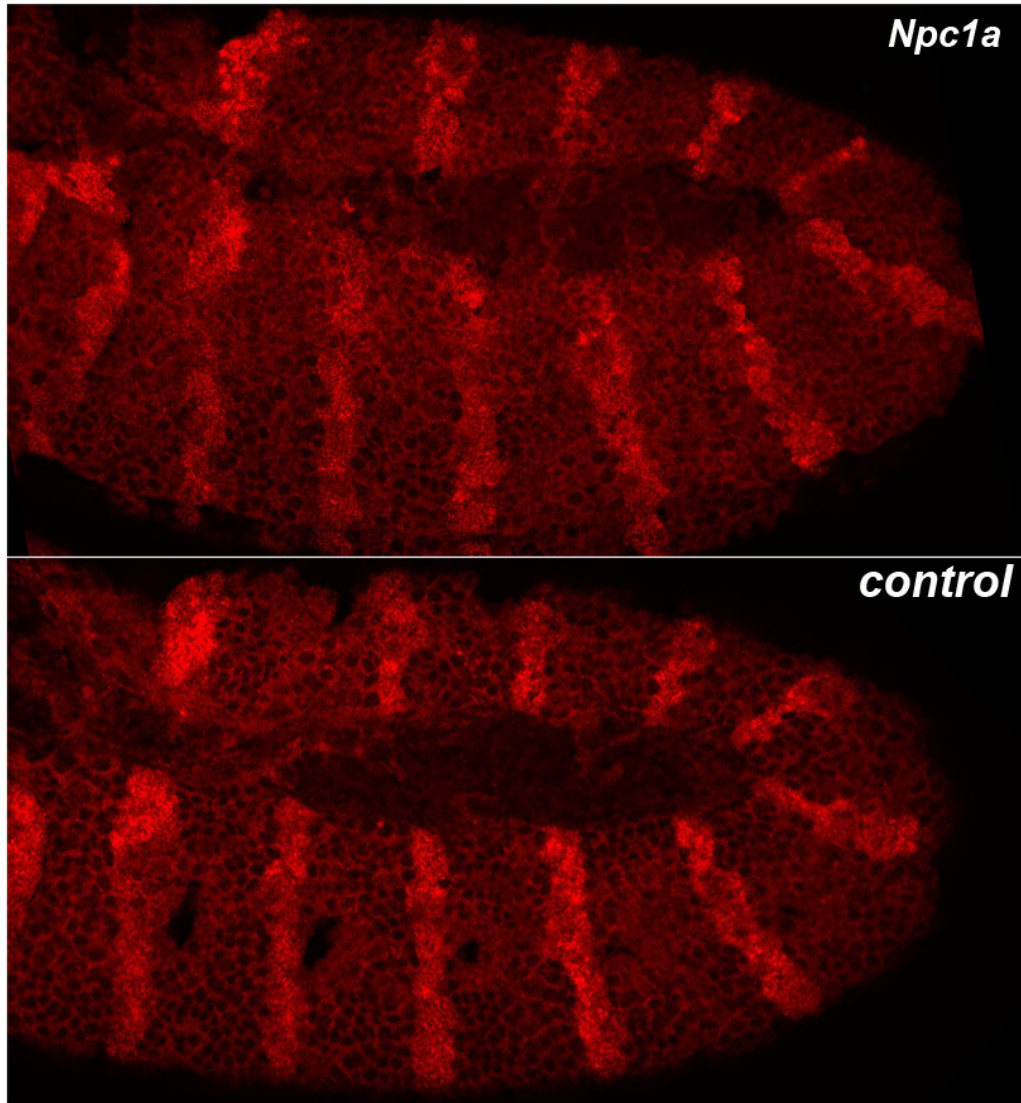


Figure S4. Engrailed expression is properly maintained in NPC1a embryos.

Embryos from the *NPC1a*^{57A}/Cy0, *en:LacZ* stock were collected and fixed using standard procedure. Embryos were genotyped by simultaneously staining them with β -galactosidase (imaged in green: not shown) and En (imaged in red) antibodies. Both control (*Balancer*) and mutant embryos show strong En specific expression in 14 stripes. Pixel intensities were compared between several pairs of embryos at identical stage and no significant difference in En (or Wg; not shown) protein levels was observed.

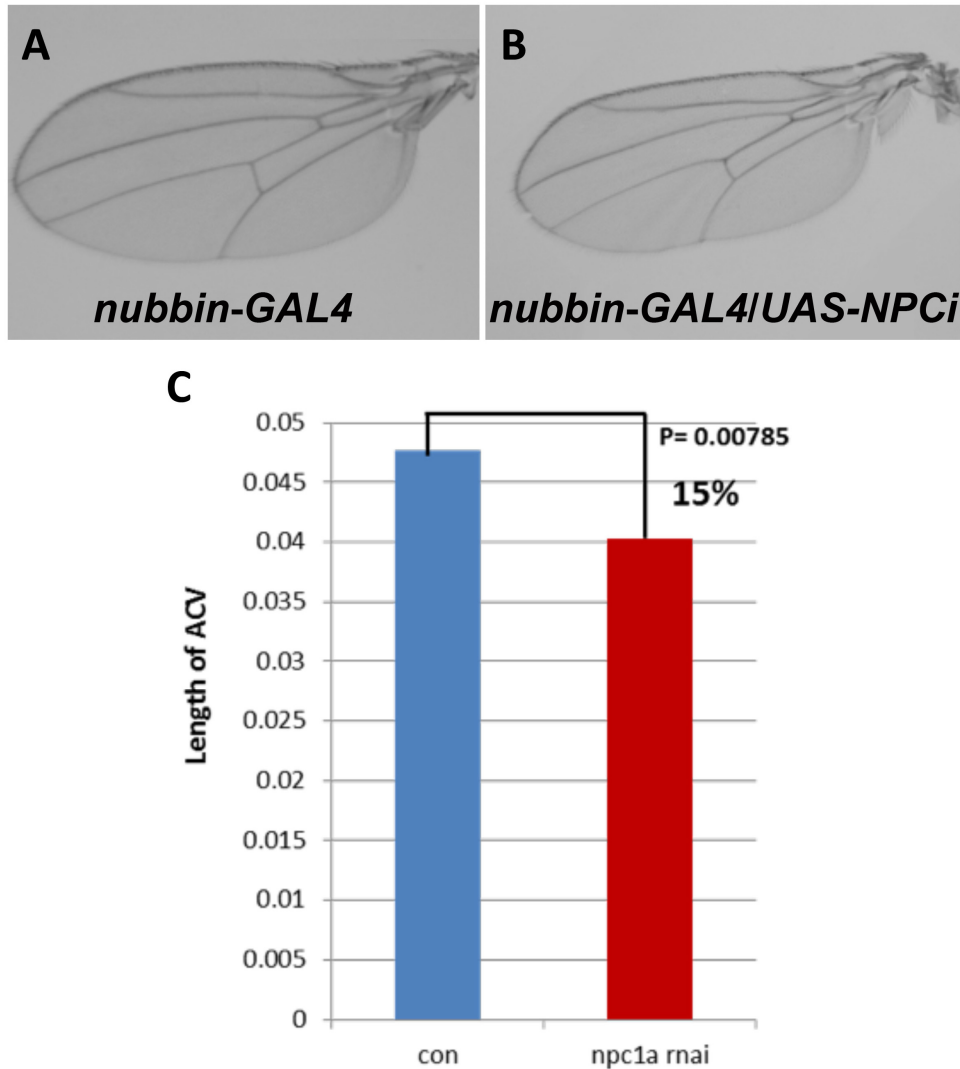


Figure S5. Compromised levels of NPC1a result in adult wing abnormalities characteristic of reduced Hh signaling.

UAS-dicer; nub-Gal4 flies were mated with *UAS-NPC1a-RNAi* flies. Panels A and B show adult wings of the specified genotypes.

(A): *UAS-dicer; nubbin-GAL4; UAS-GFP*.

(B): *UAS-dicer; nubbin-GAL4/UAS-NPC1a-RNAi; UAS-NPC1a-RNAi*.

(C): Relative estimation of the average length of the anterior cross vein (ACV) from the control and NPC1a knockdown adult wings. (n=60, three independent trials were conducted).